Effect of Molecular Weight of Polyethylene Glycol on the Equilibrium Dissociation Pressures of Methane Hydrate System

ARTICLE *in* JOURNAL OF CHEMICAL & ENGINEERING DATA · MAY 2015

Impact Factor: 2.04 · DOI: 10.1021/acs.jced.5b00088

3 AUTHORS:

Deepjyoti Mech

Indian Institute of Technology Madras

9 PUBLICATIONS **7** CITATIONS

SEE PROFILE

Gaurav Pandey

Indian Institute of Technology Madras

4 PUBLICATIONS **2** CITATIONS

SEE PROFILE

Jitendra Sangwai

Indian Institute of Technology Madras

62 PUBLICATIONS **205** CITATIONS

SEE PROFILE

Journal of chemical & engineering data

Article

pubs.acs.org/jced

Effect of Molecular Weight of Polyethylene Glycol on the Equilibrium Dissociation Pressures of Methane Hydrate System

Deepjyoti Mech, Gaurav Pandey, and Jitendra S. Sangwai*

Gas Hydrate and Flow Assurance Laboratory, Petroleum Engineering Program, Department of Ocean Engineering, Indian Institute of Technology Madras, Chennai 600 036, India

ABSTRACT: The experimental phase equilibrium data for methane (CH_4) clathrate hydrates in the presence of polyethylene glycol (PEG) aqueous solutions with various number-average molecular weights of 200 kg/kmol (PEG-200), 400 kg/kmol (PEG-400), and 600 kg/kmol (PEG-600) for (0.077, 0.2, 0.4, 0.44 and 0.46) mass fractions at the temperature range (270.75 to 281.45) K and pressure range (4.60 to 7.05) MPa has been reported. The isochoric pressure-search method is used to generate the equilibrium data on the hydrate system. Comparative effects of PEG-200, PEG-400, and PEG-600 aqueous solutions at various concentrations (mass fraction and mole fraction basis) on the methane hydrate system have been studied. The inhibition effect using low molecular weight PEG-200 is observed to be more effective in suppressing the methane hydrate formation than PEG-400 and PEG-600 at the same mass fraction. On the mole fraction basis, at higher concentration, the inhibition effect of PEG-600 on the methane hydrate system at the same mole fraction is observed to be more than PEG-200. Surprisingly, at lower concentration (at the same mole fraction), PEG-200 is observed to inhibit the methane hydrate system more than PEG-600. The methane hydrate suppression temperature using PEG-200, PEG-400, and PEG-600 is also determined using Hammerschmidt's equation and are reported. The work also reports the values of enthalpy of dissociation determined using the Clausius−Clapeyron equation for a methane hydrate system in the presence of PEG-200, PEG-400, and PEG-600 aqueous solutions. The enthalpy of dissociation of methane hydrate is observed to increase with increasing molecular weight of PEG. The study shows the effectiveness of low molecular weight PEG in inhibiting methane hydrate as compared to higher molecular weight, thus indicating their possible use for effective design of drilling and completion fluids for hydrate bearing formation.

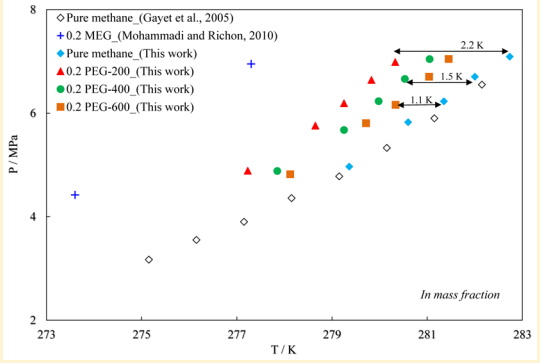

INTRODUCTION

Gas hydrates or clathrate hydrates are made up of a crystalline lattice of water molecules (host) in which gas molecules (guests) reside within water cavities made up of hydrogen-bonded water molecules.[1] Gas hydrates typically form at high pressure and low temperature conditions in the presence of guest gases such as, carbon dioxide (CO_2), nitrogen (N_2), hydrogen sulfide (H_2S), and other hydrocarbons gases such as methane (CH_4), ethane (C_2H_6), etc. Basic known hydrate structures are structure-I, structure-II, and structure-H. Among these three structures, structure I is mostly found to have cages which are made up of body-centered packing, having more spaces to include methane (CH_4), ethane (C_2H_6), and other gases such as, CO_2, H_2S, etc., of around similar molecular diameter.[1] The formation of gas hydrates is a significant problem for flow assurance in the upstream oil and gas industry. It is very difficult to remove the hydrate plug once formed in the flowline, and a plug may lead to collapse of the oil and gas production system. Once the hydrates are formed in the oil and gas transporting pipelines, it may lead to an increase in flow pressure drop, flow path blockage, and sometimes may cause the pipeline to explode causing injury and increase in the loss-time and legal costs for the industry.[2] In addition hydrocarbons and nonhydrocarbons may easily react chemically with the pipeline surface during hydrate formation corroding the pipe.[3,4]

Gas hydrates also pose a major threat when an oil or gas well is drilled, particularly in offshore environments. During the drilling operation, if the drill bit encounters an unknown hydrate zone, the drilling of the same may result in a sudden hydrate dissociation leading to increase in in situ gas pressure combined with increased drill bit temperature. The dissociated gas may also get circulated along with the drilling fluids, which may also reform as hydrate thus blocking the drilling pipe resulting in terminating the drilling fluid circulation.[5] This may affect wellbore instability, widening of the wellbore, casing running difficulties, drilling fluid gasification, formation failure, and increased operational and personnel health risks.[6] Gas hydrate dissociation is another concern of risk during wellbore casing cementing.

In recent years, the petroleum industry has accelerated the pace of hydrocarbon exploitation with increased drilling operations in deep-offshore. Because of this, the problems related hydrate formation during drilling in offshore environ-

Received: January 28, 2015
Accepted: May 12, 2015
Published: May 20, 2015

DOI: 10.1021/acs.jced.5b00088
J. Chem. Eng. Data 2015, 60, 1878−1885

ments should be taken into consideration. Two drilling accidents have been reported by Barker et al.[7] involving gas hydrate formation in drilling fluids. The first, at Santa Barbara, California, and the second at Green Canyon in the Gulf of Mexico. Birchwood et al.[8] concluded that on decreasing the circulation rate and cooling of a drilling fluid, the effect of drilling through gas-hydrate-bearing formation during hydrocarbon exploitation can be minimized. Indeed, it is important to take appropriate measures to inhibit the formation of gas hydrate or minimize gas-hydrate dissociation within the drill string or annulus to ensure safety in drilling operations.[9] Thus, the proper design of drilling fluids is an important precursor in achieving the above-mentioned objectives.

Recently, chemical additives have been developed to design an effective drilling fluid system so as to prevent the hydrate plugging in the oil and gas transporting pipelines. These chemicals behave like thermodynamic inhibitors and low-dosage hydrate inhibitors to prevent hydrate formation conditions.[2,10] The thermodynamic hydrate inhibitors are used to inject at the wellhead or in pipelines to suppress the hydrate equilibrium curve so as to have the operating conditions of flowlines away from the hydrate forming conditions. It is expected that the inhibitor molecule would compete with the water molecule by changing the chemical potential of hydration, which changes the thermodynamic equilibrium conditions of water and gas molecules avoiding hydrate formation.[11,12] For suppression of hydrate formation, thermodynamic hydrate inhibitors such as methanol and monoethylene glycol (frequently known as glycol, ethylene glycol, or MEG) are commonly used because they are more reliable and well proven.[13,14] On a mass basis, methanol is the most efficient, inexpensive, and easily available, but it is also a volatile chemical, losses to the gas phase are more, complications may arise during handling because of its toxicity and flammability, and also its use as an additive in drilling fluid design will not add value to the properties of the drilling fluid.[15] On the other side, MEG is less volatile and can be recirculated after use, may also help to displace water from clay cuttings, reducing swelling pressure, maintaining cuttings integrity, has low toxicity and is less flammable than methanol.[15,16]

At present, offshore drilling operations are using a polymer-based drilling fluid system of suitable viscosity which contains salts and organic agents and are well-known as thermodynamic hydrate inhibitors. In recent years, there has been a great interest to develop a water-soluble polymer as kinetic hydrate inhibitor for various reasons.[17,18] Among polymers, which are used in the drilling fluid, polyethylene glycols (PEG) may have significant impact on gas hydrate phase stability and has not yet been investigated in detail. PEG is also observed to be good at intercalating within the clay matrix to keep the drilled cuttings intact and firm which reduces the mud maintenance cost and waste volumes. PEG also helps to reduce the fluid loss at high temperatures, improves drilling fluid properties, and is less toxic and easily biodegradable as far as being an environmental hazard is concerned.[5,19] The information on the methane hydrate phase stability conditions in the presence of PEG are vital for their use in the development of suitable drilling fluids for hydrate bearing formations.

In this work, equilibrium data on the phase stability with three phases, hydrate−liquid water−vapor (H−L_w−V) of methane (CH_4) clathrate hydrates in the presence of PEG with number-average molecular weight of 200 kg/kmol, 400 kg/kmol, and 600 kg/kmol (viz., PEG-200; PEG-400, and PEG-600) are reported at different pressure conditions. In addition, the effect of the molecular weight of PEG (PEG-200, PEG-400, and PEG-600) on the ternary methane hydrate system is investigated for (0.077, 0.2, 0.4, 0.44, and 0.46 mass fractions) of aqueous solutions. The phase equilibrium values were reported for a temperature range (270.75 to 281.45) K and pressure range (4.60 to 7.09) MPa. The heat of dissociation H_{diss} (kJ/mol) is also reported here which is determined from the Clausius−Clapeyron equation for various concentrations of PEG for methane hydrate system.

EXPERIMENTAL STUDY

Materials. Table 1 show the materials along with their suppliers and purity in mass fraction used in this experimental study. Table 2 shows the properties of the PEGs used in this experimental study. Aqueous solutions were prepared gravimetrically using an analytical balance (Radwag AS-220/X) with an uncertainty of ± 0.00004 mass fraction.

Table 1. Suppliers of Materials Used for the Hydrate Phase Stability Study along with their Mass Fraction Purity[a]

chemical	supplier	purity mass fraction
methane	Bhuruka Gas Agency, Banglore	0.995
polyethylene glycol (PEG-200)	Merck, Mumbai	> 0.99
polyethylene glycol (PEG-400)	Merck, Mumbai	> 0.99
polyethylene glycol (PEG-600)	Merck, Mumbai	> 0.99

[a]Deionized water was used in all the experiments.

Table 2. Properties of PEG Used in This Work

property	PEG-200	PEG-400	PEG-600
mean molecular weight[a]	190 to 210	380 to 420	570 to 630
viscosity at 100 °C (CSt)[b]	4.3	7.3	10.8
flash point (°C)[b]	185	227	185
freezing point (°C)[b]	−65	4 to 8	16 to 26
density (g/cm^3) at 20 °C[a,b]	1.124	1.125	1.126
toxicity−human hazard[b]	nonhazardous	nonhazardous	nonhazardous

[a]From the supplier. [b]Reference 19.

Experimental Setup. The schematic of the experimental setup used in this work is shown in Figure 1.[20,21] The setup consists of a high pressure reactor made up of a stainless steel vessel (SS-316) with a capacity of 1.4 L and a working pressure up to 10 MPa. A platinum resistance thermometer (Pt-100) and pressure transducer are enclosed within the reactor. The dead weight pressure testing equipment is used for the calibration of pressure transducer in the range of 1 MPa to 7 MPa. According to DIN 43760, the temperature sensor (Pt-100) is class A type and calibrated through American Society for Testing and Materials (ASTM) 1137 procedure prior to use. An uncertainty of the instrument is ± 0.005 MPa and ± 0.05 K for pressure and temperature, respectively. To facilitate the gas−liquid interface, a high performance magnetic stirrer is

DOI: 10.1021/acs.jced.5b00088
J. Chem. Eng. Data 2015, 60, 1878−1885

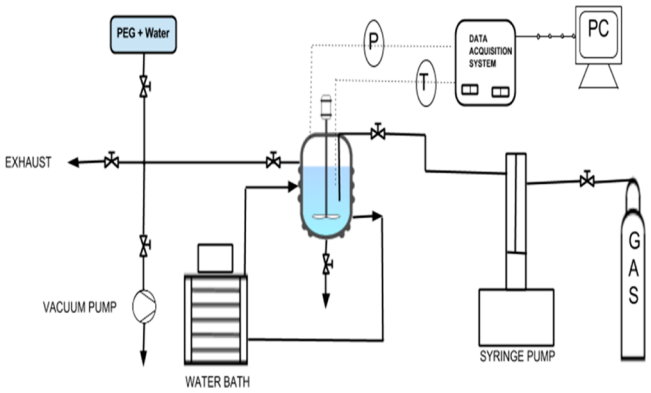

Figure 1. Schematic diagram of the experimental setup used for gas hydrate studies.

employed within a speed range of 200 rpm to 1000 rpm (revolutions per minute) which helps to reach the equilibrium. The speed of the magnetic stirrer is maintained around 400 rpm throughout all the experimental runs. Sufficient agitation is provided using this speed to ascertain the liquid phase metastability in the region of thermodynamic hydrate stability as well as to reduce the mass and heat transfer resistances by limiting the rate of hydrate formation and dissociation. A jacket is placed around the reactor to maintain the temperatures of the experimental study with the help of a Julabo water bath (model FP 50-HL) which is used for circulation of the water−glycol mixture as a heat/cold carrier. Evacuation of atmospheric gases from the reactor is done by using a vacuum pump prior to adding a PEG aqueous solution to the reactor. A D-series Syringe Pump (Teledyne ISCO, model 500D) with a capacity of 507.38 mL is used to transfer methane gas from a cylinder to the reactor with a sufficient flow rate to attain a desirable starting pressure for hydrate formation in the reactor.

Experimental Procedure. In this study, the high pressure reactor (as shown in Figure 1) is thoroughly cleaned before use. A 600 mL sample of various concentrations of PEG aqueous solutions (PEG-200, PEG-400, PEG-600) as listed in Table 3 is filled in the reactor. First, the reactor is preflushed at least twice with methane gas at about 0.1 MPa to ensure that no dissolved or free air remains inside the reactor system. Subsequently, the reactor is pressurized with methane gas up to a desired pressure using a syringe pump. To make gas−liquid contact, the reactor system is stirred at 400 rpm and the temperature is allowed to decrease to form hydrate by circulating the cold fluid around the jacket surrounding the reactor. The equilibrium conditions for the three phase (H−L_w−V) system are determined using an isochoric pressure-search method.[16,22] Various isochors were generated to obtain the equilibrium data for different initial pressure and temperature conditions and all are not reported here for the sake of simplicity. A sample isochor is shown in Figure 2 for the case of methane gas hydrate in an aqueous solution of 0.2 mass fraction polyethylene glycol (PEG-200). As shown in Figure , as the reactor temperature starts to decrease, the pressure is also decreased (from point a to point b) because of cooling of the reaction mass. Indication of hydrate formation inside the vessel is shown by a sharp decrease in pressure with a sudden increase in temperature due to exothermicity at the onset of hydrate formation at point b. The hydrate formation continued up to point c to ensure formation of sufficient methane hydrates in the system. Subsequently, the temperature of the reactor system gradually increased at a rate of 1 K/h (from points c to d) and thereafter the system heated at a rate of 0.1 K/h to 0.2 K/h (from points d to e) using a ramp profile heating to attain an accurate equilibrium point. The ramp profile continuous heating rate at 0.1 K/h to 0.2 K/h helps to achieve a correct equilibrium point, which is observed as a sharp bend in the slope of the dissociation curve near the equilibrium point.[23] The stepwise heating also enables a correct equilibrium point as it keeps changing the temperature of the system by steps and allows the system to reach the equilibrium point by giving sufficient time after each temperature rise.[24,25] Both the procedures give identical results which match well with the known literature data, if the heating rate is sufficiently slow to achieve the equilibrium point in the system during gas hydrate dissociation which has been confirmed by Gayet et al. (2005).[22] We followed the ramp profile heating which gave satisfactory results as compared with literature data.[20,21,26] With the help of the above procedure, the pressure−temperature diagram is plotted for each experimental run. The equilibrium point is determined from the intersection point between the three phase (H−L_w−V) dissociation line and the two phase contraction line of the fluid mixture (V−L) as shown in Figure

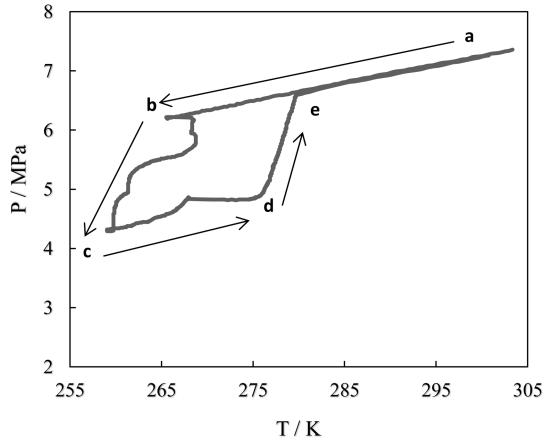

Figure 2. Isochoric pressure−temperature diagram for a sample methane hydrate system in 0.2 mass fraction PEG-200 aqueous solution.

Table 3. Details of the Various Concentrations (Mass Fraction and Mole Fraction) of Polyethylene Glycol (PEG-200, PEG-400, and PEG-600) in Aqueous Solution for the Range of Equilibrium Pressure, *P*, and Temperature, *T*, Generated in This Work for Methane Gas Hydrate

aqueous solution system	mass fraction	mole fraction	methane hydrate dissociation temperature range/K	methane hydrate dissociation pressure range/MPa
pure methane	nil	nil	(279.36 to 282.73)	(4.97 to 7.09)
PEG-200	0.077	0.007	(277.95 to 281.25)	(4.86 to 7.05)
	0.2	0.022	(277.23 to 280.33)	(4.89 to 6.99)
	0.4	0.055	(271.75 to 275.49)	(4.60 to 6.99)
	0.46	0.07	(270.75 to 272.05)	(5.53 to 6.36)
PEG-400	0.2	0.01	(277.85 to 281.05)	(4.88 to 7.04)
	0.4	0.028	(274.06 to 276.95)	(4.82 to 6.87)
PEG-600	0.2	0.007	(278.12 to 281.45)	(4.82 to 7.05)
	0.4	0.02	(274.03 to 277.69)	(4.69 to 6.93)
	0.44	0.022	(273.25 to 276.95)	(4.68 to 6.83)

DOI: 10.1021/acs.jced.5b00088
J. Chem. Eng. Data 2015, 60, 1878−1885

Table 4. Experimental Equilibrium Data with Their Dissociation Enthalpies for Methane Hydrates in the Presence of Polyethylene Glycol (PEG-200, PEG-400 and PEG-600) in Aqueous Solutions

aqueous solution system	mass fraction	mole fraction	T[a] (K)	P[b] (MPa)	Clausius–Clapeyron, H_{diss} (kJ/mol)
pure methane hydrate	nil	nil	279.36	4.97	62.38
			280.60	5.83	61.44
			281.35	6.23	61.06
			282.00	6.70	60.60
			282.73	7.09	60.29
PEG-200	0.077	0.007	277.95	4.86	66.09
			277.95[c]	4.91[c]	66.01
			279.35	5.48	65.39
			280.15	6.21	64.55
			280.55[c]	6.49[c]	64.25
			280.65	6.58	64.16
			281.15	7.04	63.69
			281.25[c]	7.05[c]	63.69
	0.2	0.022	277.23	4.89	64.69
			278.61[c]	5.78[c]	63.64
			278.65	5.76	63.67
			279.24[c]	6.21[c]	63.17
			279.25	6.19	63.20
			279.68[c]	6.58[c]	62.78
			279.83	6.64	62.73
			280.16[c]	6.93[c]	62.43
			280.33	6.99	62.38
	0.4	0.055	271.75	4.60	58.39
			273.45	5.54	57.30
			274.05	5.90	56.91
			274.65	6.32	56.46
			275.49	6.99	55.79
	0.46	0.07	270.75	5.53	51.84
			271.45	5.92	51.44
			272.05	6.36	51.00
PEG-400	0.2	0.01	277.85	4.88	71.07
			279.25	5.67	70.07
			279.98	6.23	69.40
			280.53	6.66	68.91
			281.05	7.04	68.51
	0.4	0.028	274.06	4.82	58.23
			275.80	5.68	57.31
			276.15	5.96	57.00
			276.69	6.30	56.66
			276.95	6.87	56.04
PEG-600	0.2	0.007	278.12	4.82	72.22
			279.72	5.81	70.95
			280.34	6.16	70.55
			281.04	6.70	69.93
			281.45	7.05	69.56
	0.4	0.02	274.03	4.69	61.82
			275.55	5.55	60.80
			276.45	6.09	60.21
			277.20	6.57	59.72
			277.69	6.93	59.36
	0.44	0.022	273.25	4.68	60.71
			273.35[c]	4.76[c]	60.60
			275.05	5.69	59.53
			275.65	6.07	59.12
			276.45[c]	6.49[c]	58.70
			276.45	6.51	58.68
			276.85[c]	6.81[c]	58.38
			276.95	6.83	58.37

[a]Expanded uncertainty in temperature = ± 0.109 K. [b]Expanded uncertainty in pressure = ± 0.021 MPa. [c]Reproduced data.

2. The equilibrium pressures and temperatures were determined with an expanded uncertainty of ± 0.109 K and ± 0.021 MPa, respectively.

RESULTS AND DISCUSSION

In this study, experimental equilibrium conditions on the pressure and temperature for methane hydrate in the presence of various systems of polyethylene glycol (PEG-200, PEG-400, and PEG-600) in an aqueous solution have been reported. Table 3 shows details on the various concentrations (mass fraction and mole fraction) of PEG-200, PEG-400, and PEG-600 aqueous solutions used for the study with the range of equilibrium pressure, *P*, and temperature, *T*, generated in this work. First, the equilibrium data on the pure methane gas hydrate system are compared with selected experimental data available in the literature to validate experimental results.[22] Table 4 shows the equilibrium temperature and pressure data for pure methane gas hydrate, and also data for the hydrate in the presence of various concentrations of PEG-200, PEG-400, and PEG-600 are plotted in Figures 3, 4, and 5. The results on the phase stability conditions for pure methane hydrate generated in this study (see Figure 3a) agree well with the literature data[22] confirming the reliability of the experimental setup and procedure adopted in this study. Figure 3 shows the phase stability conditions for methane gas hydrate in the presence of PEG-200 (Figure 3a), PEG-400 (Figure 3b), and PEG-600 (Figure 3c). Figure 3b also shows the phase stability data for methane hydrate system with PEG-400 for 0.4 mass fraction obtained from the literature.[16] Mohammadi et al.[16] carried out studies only for the PEG-400 system at 0.1 and 0.4 mass fraction. The data generated in this work for the same concentration (0.4 mass fraction) of PEG-400 agrees well with the literature value.[16] The inhibition effect on the methane hydrate is observed to increase with an increase in the concentration of PEG-200, PEG-400, and PEG-600 from 0.2 to 0.4 in the aqueous system. In general, the phase equilibrium data for the ternary gas hydrate system (H_2O + PEG + CH_4) is shifted toward lower temperatures and higher pressures as compared to the phase equilibrium data of pure CH_4 hydrate system. Figure 3 also shows selected data on the methane hydrate phase stability in the presence of 0.1 and 0.2 mass fraction of MEG from the literature[13] for comparison. For the same mass fraction (for e.g., 0.2) of MEG and PEG (see Figure 3a,b,c) MEG shows higher inhibition capacity than PEG on the methane hydrate system. However, the 0.4 mass fraction of PEG-200 is observed to inhibit methane hydrate more than the 0.2 mass fraction of MEG in an aqueous system, while the 0.1 mass fraction of MEG is shown to inhibit methane hydrate by the same magnitude as PEG-200 at the 0.2 mass fraction in an aqueous system (Figure 3a). In addition, the phase equilibrium

DOI: 10.1021/acs.jced.5b00088
J. Chem. Eng. Data 2015, 60, 1878–1885

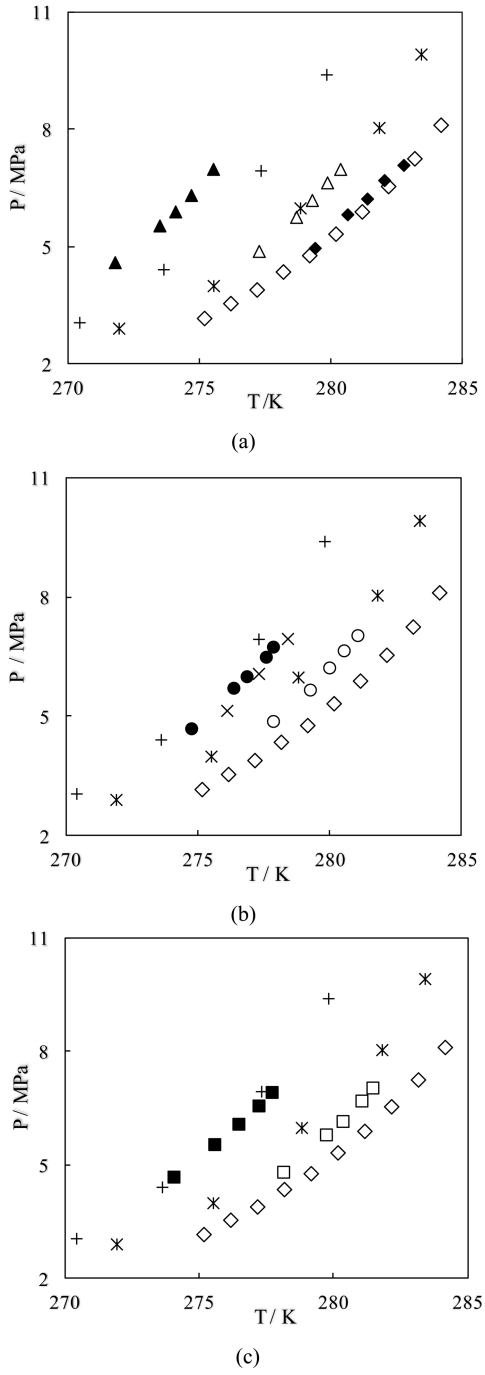

Figure 3. Phase equilibria of methane hydrate in the presence of PEG-200, PEG-400, and PEG-600 aqueous solution at 0.2 and 0.4 mass fractions. ◊, pure methane hydrate;[22] ∗, 0.1 mass fraction MEG;[13] +, 0.2 mass fraction MEG.[13] (a) ◆, Pure methane hydrate (this work); △, 0.2 mass fraction PEG-200 (this work); ▲, 0.4 mass fraction PEG-200 (this work). (b) ○, 0.2 Mass fraction PEG-400 (this work); ●, 0.4 mass fraction PEG-400 (this work); ×, 0.4 mass fraction PEG-400.[16] (c) □, 0.2 Mass fraction PEG-600 (this work); ■, 0.4 mass fraction PEG-600 (this work).

curves for PEG-400 and PEG-600 at 0.4 mass fraction are almost overlapping to that of the 0.2 mass fraction of MEG (see Figure 3b,c). However, for PEG-400 and PEG-600 at 0.2 mass fraction, the effect of inhibition on methane hydrate is slightly lower than that of the 0.1 mass fraction of MEG in an aqueous system (see Figure 3b,c).

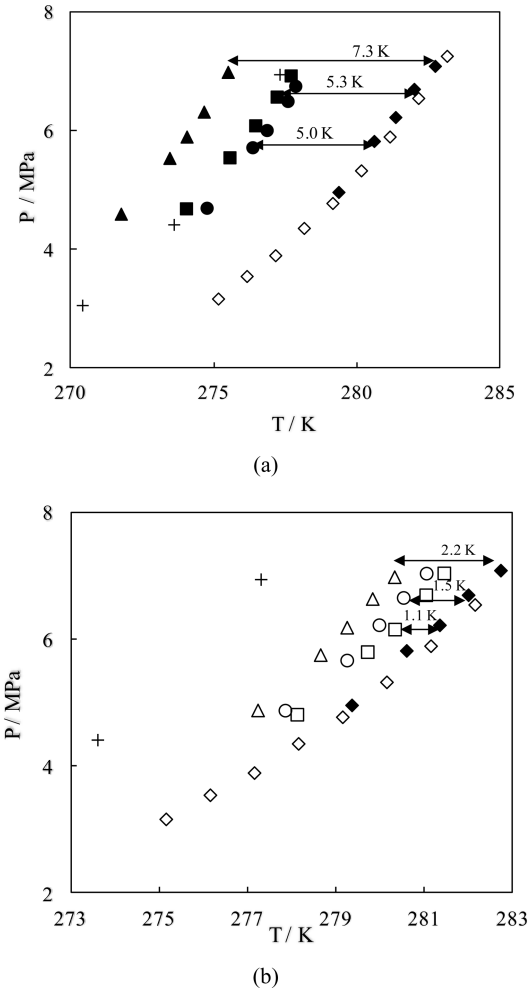

Figure 4. Phase equilibria of methane hydrate in the presence of PEG-200, PEG-400, and PEG-600 aqueous solution at 0.2 and 0.4 mass fractions. ◊, Pure methane hydrate;[22] +, 0.2 mass fraction MEG;[13] ◆, pure methane hydrate (this work). (a) ▲, 0.4 mass fraction PEG-200 (this work); ●, 0.4 mass fraction PEG-400 (this work); ■, 0.4 mass fraction PEG-600 (this work). (b) △, 0.2 mass fraction PEG-200 (this work); ○, 0.2 mass fraction PEG-400 (this work); □, 0.2 mass fraction PEG-600 (this work).

Figure 4a,b shows the comparative effect of the molecular weight of PEG (PEG-200, PEG-400, PEG-600) on the phase stability of the methane hydrate system. At the same mass fraction, say 0.4, it is observed that PEG-200 shows more inhibition on methane hydrate than PEG-400 and PEG-600 aqueous systems. The ternary hydrate systems containing (H_2O + 0.4 mass fraction PEG-400 + CH_4) and (H_2O + 0.4 mass fraction PEG-600 + CH_4) are showing almost the same inhibition on methane hydrate system. In general, the inhibition capacity of PEG on methane hydrate shows trends as, PEG-600 < PEG-400 < PEG-200. This means that as the molecular weight of PEG increases, the inhibition effect of PEG on the methane hydrate system decreases. Also, as the molecular weight of PEG decreases, the inhibition tendency of PEG on methane hydrate increases and tends toward that of the monomer MEG at the same concentration as seen in Figure 4b. Also, as shown in Figure 4a, at 0.4 mass fraction, PEG-200, PEG-400, and PEG-600 provides an average hydrate suppression temperature of around 7.3, 5.3, and 5 K, respectively. It is also observed from Figure 4b that, at 0.2

DOI: 10.1021/acs.jced.5b00088
J. Chem. Eng. Data 2015, 60, 1878−1885

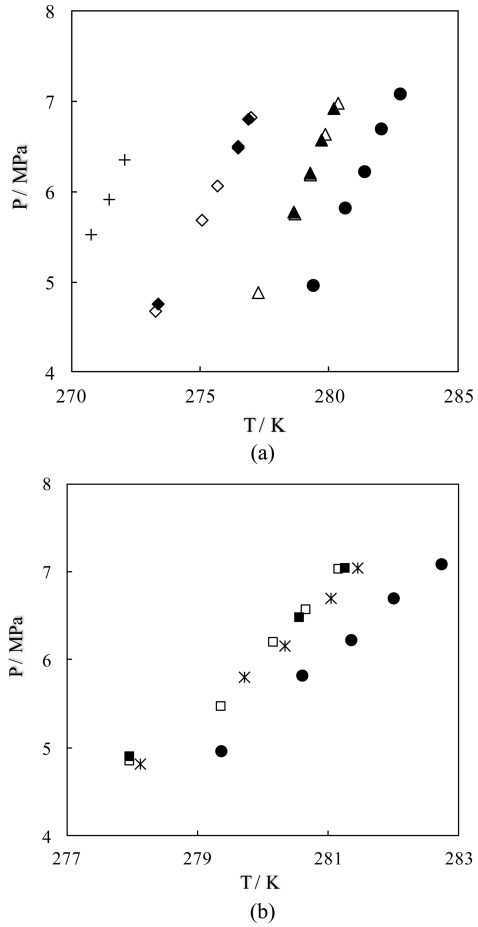

Figure 5. Phase equilibria of methane hydrate in the presence of PEG-200 and PEG-600 at various concentrations. ●, Pure methane hydrate (this work). (a) +, 0.07 mole fraction PEG-200 (0.46 mass fraction) (this work); ◊, 0.022 mole fraction PEG-600 (0.44 mass fraction) (this work); ◆, 0.022 mole fraction (0.44 mass fraction) PEG-600 reproduced (this work); ▲, 0.022 mole fraction (0.2 mass fraction) PEG-200 (this work); △, 0.022 mole fraction (0.2 mass fraction) PEG-200, reproduced (this work). (b) □, 0.007 Mole fraction (0.077 mass fraction) PEG-200 (this work); ■, 0.007 mole fraction (0.077 mass fraction) PEG-200, reproduced (this work); *, 0.007 mole fraction (0.2 mass fraction) PEG-600 (this work).

mass fraction, PEG-200, PEG-400, and PEG-600 provides hydrate suppression temperatures of about 2.2, 1.5, and 1.1 K, respectively.

An empirical formula is given by Hammerschmidt[27,28] for predicting the suppression temperature of a gas hydrate system as shown in eq 1:

$$(\Delta T)_{p\_avg} = \frac{Kx}{M(100 - x)} \quad (1)$$

where, $(\Delta T)_{p\_avg}$ is the hydrate suppression temperature (K), while K is a constant which is specific to each inhibitor, M is the molecular weight of the inhibitor, and x is the mass concentration of the inhibitor. The corresponding tuned values of K for the equilibrium data generated in this work for PEG-200, PEG-400, and PEG-600 are found to be 346805.17, 502403.12, and 464596.58, respectively. The experimental $((\Delta T)_{exp\_avg})$ and calculated hydrate suppression temperatures $((\Delta T)_{p\_avg})$ using eq 1 are tabulated in Table 5. It is observed that the Hammerschmidt's equation (1) is able to predict the hydrate suppression temperature quite satisfactorily for pressure ranges for various mass fractions of PEG-200, PEG-400, and PEG-600 for the methane hydrate system.

Table 5. Hydrate Suppression Temperature of Methane Hydrate System in the Presence of Different Molecular Weights of PEG[a]

inhibitor	mass fraction	pressure limits (MPa)	$(\Delta T)_{exp\_avg}$ (K)	$(\Delta T)_{p\_avg}$ (K)
PEG-200	0.4	4.60 to 6.99	7.33	6.72
	0.2	4.89 to 6.99	2.15	3.35
PEG-400	0.4	4.82 to 6.87	5.28	4.82
	0.2	4.88 to 7.04	1.48	2.40
PEG-600	0.4	4.69 to 6.93	5.02	3.01
	0.2	4.82 to 7.05	1.08	1.50

[a]Notation: "exp" is experimental value; 'p' is calculated value.

A study is also performed to compare the effect of molecular weight of polymer PEG on the mole fraction basis. A few sets of experiments were performed at the same mole fraction for PEG-200 and PEG-600 in an aqueous system. Table 4 and Figure 5 show the corresponding data on the phase stability of methane hydrate for same mole fraction basis (0.022 and 0.007 mole fraction). It is observed that at 0.07 mole fraction of PEG-200, the equilibrium curve shifts more toward the left as compared with 0.022 mole fraction of PEG-200 and PEG-600, which show strong inhibition. At the same concentration (0.022 mole fraction, see Figure 5a), the effect of inhibition for PEG-600 is more ($(\Delta T)_{exp\_avg}$ of 5.7 K) as compared to that of PEG-200 ($(\Delta T)_{exp\_avg}$ of 2.2 K). Interestingly, at low concentration (0.007 mole fraction, see Figure 5b), PEG-200 is suppressing more ($(\Delta T)_{exp\_avg}$ of 1.4 K) as compared with PEG-600 ($(\Delta T)_{exp\_avg}$ of 1.0 K) for methane hydrate formation. As the trends on the effect of the same molecular weight of PEG on mole fraction basis is not in order for two selected studies (0.022 and 0.007 mole fractions), the selected sets of experiments were repeated to confirm the reproducibility. Table 4 shows the equilibrium data reproduced for the above-mentioned cases and the data are also shown in Figure 5a,b, which indeed proves the reproducibility of the experimental result. Indeed, the effect of polymer on mole fraction basis may need further investigation to understand the effect of polymer molecules on methane hydrate inhibition.

The dissociation enthalpies of methane hydrate is determined for different molecular weights of PEG aqueous solution. The heat of dissociation is one of a hydrate thermal property which is important for hydrate inhibition methods.[29] The measurements of enthalpies of dissociation of gas hydrates is typically obtained using a direct calorimetric study and indirectly using the Clausius−Clapeyron and Clapeyron equation.[29] The Clausius−Clapeyron equation is given as

$$\frac{d\ln P}{d\left(\frac{1}{T}\right)} = -\frac{H_{diss}}{zR} \quad (2)$$

where P is the pressure (MPa), T is the temperature (K), z is the compressibility factor for gas and is determined through the Soave−Redlich−Kwong (SRK) equation, R is the universal gas constant, H_{diss} is the molar enthalpy of dissociation of methane gas hydrate in (kJ/mol). The plot for the concentration (0.4 mass fraction) of different molecular weight PEG-200, PEG-400, and PEG-600 has been made between ln P versus $(1/T)$ as shown in Figure 6. The ln P versus $(1/T)$ exhibits a good linear

DOI: 10.1021/acs.jced.5b00088
J. Chem. Eng. Data 2015, 60, 1878−1885

relation, which is indicated by the increase in equilibrium pressure along with the increase in equilibrium temperature.

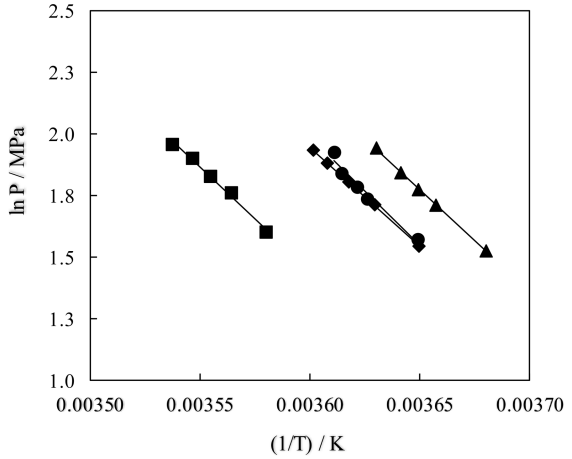

Figure 6. Semilogarithmic plots of pressure versus reciprocal temperature for CH_4 + PEG aqueous system. Experimental points: ■, pure methane hydrate (this work); ▲, 0.4 mass fraction PEG-200 (this work); ●, 0.4 mass fraction PEG-400 (this work); ◆, 0.4 mass fraction PEG-600 (this work).

Table 4 shows the dissociation enthalpies of pure methane hydrate and also in the presence of PEG aqueous solution for methane hydrate systems for different molecular weights as determined by the Clausius−Clapeyron equation from the equilibrium data. Table 4 shows that the heat of dissociation H_{diss} (kJ/mol) values have been obtained for pure methane hydrate and methane hydrate in the presence of PEG(PEG-200, PEG-400, and PEG-600) aqueous solutions from the Clausius−Clapeyron equation and are in good agreement with a literature trend.[29,30] The plot between H_{diss} (kJ/mol) vs T (K), which was determined from the Clausius−Clapeyron equation, has been shown in Figure 7. It has been observed from Figure 7 that the heat of dissociation H_{diss} (kJ/mol) obtained from the Clausius−Clapeyron equation at various concentrations (0.077, 0.2, 0.4, 0.44, and 0.46 mass fraction) for PEG-600 are higher in magnitude as compared with those for PEG-400 and PEG-200. Also for lower concentrations, say 0.077 and 0.2 mass fraction, the heat of dissociation H_{diss} (kJ/mol) is higher in magnitude as compared to that for higher concentrations, say 0.4, 0.44, and 0.46 mass fractions for PEG-200, PEG-400, and PEG-600 systems. Eventually, it is observed that as the concentration decreases for PEG-200, PEG-400, and PEG-600 in methane hydrate systems, the heat of dissociation H_{diss} (kJ/mol) is increased. Overall, the heat of dissociation shows decreasing trend as PEG-600 > PEG-400 > PEG-200. In general, the greater is the inhibition; the less is the heat of dissociation required for the methane hydrate system. The heat of dissociation H_{diss} (kJ/mol) is higher in the case of methane hydrate in the presence of tetrahydrofuran (THF) promoter[26] as compared with the inhibitors (PEG-200, PEG-400, and PEG-600) at various concentrations possibly due to the interaction between guest gas molecules and host water molecules which is known to affect the molar enthalpy of dissociation of the gas hydrate.[31]

In the aforesaid discussion, the inhibition effect of different molecular weights of PEG-200, PEG-400, and PEG-600 (on mass fraction and mole fraction basis) on the phase stability of CH_4 hydrate with different aqueous solutions is enunciated.

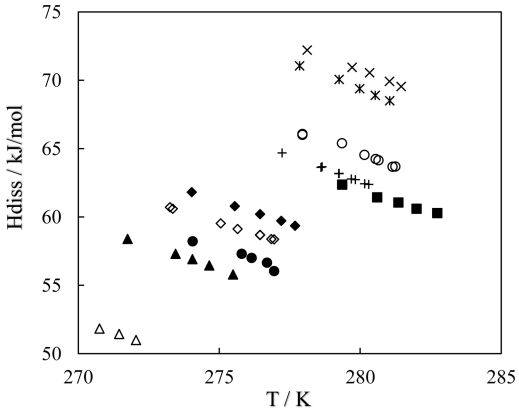

Figure 7. Plot between heat of dissociation H_{diss} (kJ/mol) and temperature, T (K) for CH_4 hydrate+PEG aqueous system. Experimental points: Clausius−Clapeyron equation ■, Pure methane (this work); ○, 0.077 mass fraction (0.007 mole fraction) PEG-200 (this work); +, 0.2 mass fraction (0.022 mole fraction) PEG-200 (this work); ∗, 0.2 mass fraction (0.01 mole fraction) PEG-400 (this work); ×, 0.2 mass fraction (0.007 mole fraction) PEG-600 (this work); ▲, 0.4 mass fraction (0.055 mole fraction) PEG-200 (this work); △, 0.46 mass fraction (0.07 mole fraction) PEG-200 (this work); ●, 0.4 mass fraction (0.028 mole fraction) PEG-400 (this work); ◆, 0.4 mass fraction (0.02 mole fraction) PEG-600 (this work); ◊, 0.44 mass fraction (0.022 mole fraction) PEG-600 (this work).

Although the inhibition effect of PEG is less than that of MEG on methane hydrate at the same concentration but as per drilling activities are concerned, the incorporation of appropriate concentrations of PEG in drilling fluid may help to have better hydrate inhibition along with better control on fluid loss properties and the viscosity of drilling fluids at reasonably high temperatures. Also, PEG shows relatively lower freezing point of −65 °C[19] as compared to MEG (freezing point of −13.4 °C), thus making PEG more useful for drilling in low temperature or permafrost hydrate zones. Moreover, the heat of dissociation is more at low concentration as compared with high concentration of PEG, and thus less heat is required to dissociate a hydrate using low molecular weight polymer for drilling hydrate zones. The phase equilibrium data, which are generated in this study, will be useful for inhibiting the methane hydrate formation in both onshore and offshore environments for efficient drilling activities.

■ CONCLUSIONS

In this work, phase equilibrium data are reported on the methane hydrate system in PEG aqueous solutions for various mass fractions. It is found that the low molecular weight polymer PEG-200 shows more inhibition than PEG-400 and PEG-600 on methane hydrate system. In addition, with increase in concentration of PEG (PEG-200, PEG-400, and PEG-600) aqueous solutions in methane hydrate system, the inhibition effect has increased. At same mole fraction, for higher concentration (0.022 mole fraction), the effect of inhibition for PEG-600 has been observed to be more than that for PEG-200. Surprisingly, at lower concentration (0.007 mole fraction), for the same mole fraction, PEG-200 is observed to suppress the formation of methane hydrate more than PEG-600. The enthalpy of dissociation is observed to be lower for the low molecular weight polymer, which indicated their efficient use as an inhibiting solution for the methane hydrate system. Though PEG shows lower inhibition than monomer MEG, it has the

DOI: 10.1021/acs.jced.5b00088
J. Chem. Eng. Data 2015, 60, 1878−1885

advantage over its use for efficient drilling and completion fluid design for hydrate bearing formations. PEG is one of the components used in drilling fluids. Alternatively, there is also a need to develop hydrate inhibiting completion fluids. The use of PEG will aid in the development of these systems if used appropriately. Presently, we are working on developing polymer systems with tuned properties (including molecular weight) for application related to polymer flooding in hydrate formation for production of methane (patent pending). We are also working on the PEG mixed with kinetic inhibitors for hydrate inhibition.

AUTHOR INFORMATION

Corresponding Author

*E-mail: jitendrasangwai@iitm.ac.in. Tel.: +91-44-2257-4825. Fax: +91-44-2257-4802.

Notes

The authors declare no competing financial interest.

REFERENCES

(1) Sloan, E. D.; Koh, C. A. *Clathrate Hydrates of Natural Gases*, 3rd ed., CRC Press, Taylor & Francis Group: Boca Raton FL, 2008.
(2) Zarinabadi, S.; Samimi, A. Problems of Hydrate Formation in Oil and Gas Pipes Deals. *Aus. J. Basic Appl. Sci.* **2011**, *5*, 741.
(3) Obanijesu, E. O.; Pareek, V.; Tade, M. O. Hydrate Formation and Its Influence on Natural Gas Pipeline Internal. Oil and Gas India Conference & Exhibition, Mumbai, India, SPE 128544, 2010.
(4) Nengkoda, A.; Reerink, H.; Hase, A.; Prasetyo, I.; Purwono, S. Hydrate Problems in Gas Lift Production: Experiences and Integrated Inhibition. Kuwait International Petroleum Conference & Exhibition, Kuwait City, Kuwait, SPE 126323, 2009.
(5) Jiang, G.; Lin, T.; Ning, F.; Tu, Y.; Zhang, L.; Yu, Y.; Kuang, L. Polyethylene Glycol Drilling Fluid for Drilling in Marine Gas Hydrates-Bearing Sediments: An Experimental Study. *Energies* **2011**, *4*, 140−150 DOI: 10.3390/en4010.
(6) Fereidounpour, A.; Vatani, A. An Investigation of Interaction of Drilling Fluids with Gas Hydrates in Drilling Hydrate Bearing Sediments. *J. Nat. Gas Sci. Eng.* **2014**, *20*, 422.
(7) Barker, J. W.; Gomez, R. K. Formation of Hydrates during Deepwater Drilling Operations. *J. Petrol. Technol.* **1989**, *41*, 297.
(8) Birchwood, R. A.; Noeth S.; Tjeengdrawira, M. A.; Kisra, S. M.; Elisabeth, F. L.; Sayers, C. M.; Singh; Hooyman P. J.; Plumb, R. A.; Jones, E.; Bloys, J. B. Modeling the Mechanical and Phase Change Stability of Wellbores Drilled in Gas Hydrates. Technical Report for Joint Industry Participation Program (JIPP) Gas Hydrates Project, Phase II: Anaheim, CA, USA, November 2007.
(9) Liyi, C.; Sheng, W.; Changwen, Y. Effect of Gas Hydrate Drilling Fluids Using Low Solid Phase Mud System in Plateau Permafrost. *Procedia Eng.* **2014**, *73*, 318.
(10) Paez, J. E.; Blok, R.; Vaziri, H.; Islam, M. R. Problems in Gas Hydrates: Practical Guidelines for Field Remediation. Latin American and Carribean Petroleum Engineering Conference, Buenos Aires, Argentina, SPE 69424, 2001.
(11) Cha, M.; Shin, K.; Kim, J.; Chang, D.; Seo, Y.; Lee, H.; Kang, S. Thermodynamic and Kinetic Hydrate Inhibition Performance of Aqueous Ethylene Glycol Solutions for Natural Gas. *Chem. Eng. Sci.* **2013**, *99*, 184.
(12) Wu, M.; Wang, S.; Liu, H. A Study on Inhibitors for the Prevention of Hydrate Formation in Gas Transmission Pipeline. *J. Nat. Gas Chem.* **2007**, *16*, 81.
(13) Mohammadi, A. H.; Richon, D. Phase Equilibria of Methane Hydrates in the Presence of Methanol and/or Ethylene Glycol Aqueous Solutions. *Ind. Eng. Chem. Res.* **2010**, *49*, 925.
(14) Ng, H.-J.; Robinson, D. B. *Gas Proc. Assoc. Res. Rep.* 1983, *66*.
(15) Fadnes, F. H.; Jakobsen, T.; Bylov, M.; Holst, A.; Downs, J. D. European Petroleum Conference, The Hague, The Netherlands, SPE 50688, 1988.
(16) Mohammadi, A. H.; Laurens, S.; Richon, D. Experimental Study of Methane Hydrate Phase Equilibrium in the Presence of Polyethylene Glycol-400 Aqueous Solution. *J. Chem. Eng. Data* **2009**, *54*, 3118.
(17) Kelland, M. A. History of the Development of Low Dosage Hydrate Inhibitors. *Energy Fuels.* **2006**, *20*, 825.
(18) Chua, P. C.; Saeb$_{Ø}$, M.; Lunde, A.; Kelland, M. A. Dual Kinetic Hydrate Inhibition and Scale Inhibition by Polyaspartamides. *Energy Fuels.* **2011**, *25*, 5165.
(19) Kaminski, L.; Downs, J. D.; Howard, S. K. 20th SPE Bergen One Day Seminar. SPE, Bergen, Norway, April 10, 2013.
(20) Godishala, K. K.; Sangwai, J. S.; Sami, N. A.; Das, K. Phase Stability of Semiclathrate Hydrates of Carbon Dioxide in Synthetic Sea Water. *J. Chem. Eng. Data* **2013**, *58*, 1062.
(21) Sami, N. A.; Das, K.; Sangwai, J. S.; Balasubramanian, N. Phase Equilibria of Methane and Carbon Dioxide Clathrate Hydrates in the Presence of (Methanol + $MgCl_2$) and (Ethylene Glycol + $MgCl_2$). *J. Chem. Thermodyn.* **2013**, *65*, 198.
(22) Gayet, P.; Dicharry, C.; Marion, G.; Graciaa, A.; Lachaise, J.; Nesterov, A. Experimental Determination of Methane Hydrate Dissociation Curve up to 55 MPa by Using a Small Amount of Surfactant As Hydrate Promoter. *Chem. Eng. Sci.* **2005**, *60*, 5751.
(23) Sangwai, J. S.; Oellrich, L. Phase Equilibrium of Semiclathrate Hydrates of Methane in Aqueous Solutions of Tetra-n-butyl Ammonium Bromide (TBAB) and TBAB-NaCl. *Fluid Phase Equilib.* **2014**, *367*, 95.
(24) Masoudi, R.; Tohidi, B.; Anderson, R.; Burgass, R. W.; Yang, J. Experimental Measurement and Thermodynamic Modelling of Clathrate Hydrate Equilibria and Salt Solubility in Aqueous Ethylene Glycol and Electrolyte Solutions. *Fluid Phase Equilib.* **2004**, *219*, 157.
(25) Tohidi, B.; Burgass, R. W.; Danesh, A.; Østergaard, K. K.; Todd, A. C. Improving the Accuracy of Gas Hydrate Dissociation Point Measurements. *Ann. N.Y. Acad. Sci.* **2000**, *912*, 924.
(26) Mech, D.; Sangwai, J. S. Phase Stability of Hydrates of Methane in Tetrahydrofuran Aqueous Solution and the Effect of Salt. *J. Chem. Eng. Data* **2014**, *59*, 3932.
(27) Hammerschmidt, E. G. Formation of Gas Hydrates in Natural Gas Transmission Lines. *Ind. Eng. Chem.* **1934**, *26*, 851.
(28) Joshi, A.; Mekala, P.; Sangwai, J. S. Modeling Phase Equilibria of Semiclathrate Hydrates of CH_4, CO_2, and N_2 in Aqueous Solution of Tetra-*n*-Butyl Ammonium Bromide. *J. Nat. Gas Chem.* **2012**, *21*, 459.
(29) Gupta, A.; Lachance, J.; Sloan, E. D., Jr.; Koh, C. A. Measurements of Methane Hydrate Heat of Dissociation Using High Pressure Differential Scanning Calorimetry. *Chem. Eng. Sci.* **2008**, *63*, 5848.
(30) Sabil, K. M.; Nasir, Q.; Partoon, B.; Seman, A. A. Measurement of H−Lw−V and Dissociation Enthalpy of Carbon Dioxide Rich Synthetic Natural Gas Mixtures. *J. Chem. Eng. Data* **2014**, *59*, 3502.
(31) Kwon, T.; Kneafsey, T. J.; Rees, E. V. L. Thermal Dissociation Behaviour and Dissociation Enthalpies of Methane−Carbon Mixed Hydrates. *J. Phys. Chem. B* **2011**, *115*, 8169.

DOI: 10.1021/acs.jced.5b00088
J. Chem. Eng. Data 2015, 60, 1878−1885